



## **UWL REPOSITORY**

**repository.uwl.ac.uk**

Extracellular ph monitoring for use in closed-loop vagus nerve stimulation

Cork, Simon, Eftekhari, Amir, Mirza, Khalid, Zuliani, Claudio, Nikolic, Konstantin ORCID logo ORCID: <https://orcid.org/0000-0002-6551-2977>, Gardiner, James, Bloom, Stephen and Toumazou, Christofer (2018) Extracellular ph monitoring for use in closed-loop vagus nerve stimulation. Journal of neural engineering, 15 (1). 016001. ISSN 1741-2560

<http://dx.doi.org/10.1088/1741-2552/aa8239>

This is the Published Version of the final output.

UWL repository link: <https://repository.uwl.ac.uk/id/eprint/7975/>

**Alternative formats:** If you require this document in an alternative format, please contact: [open.research@uwl.ac.uk](mailto:open.research@uwl.ac.uk)

**Copyright:** Creative Commons: Attribution 3.0

Copyright and moral rights for the publications made accessible in the public portal are retained by the authors and/or other copyright owners and it is a condition of accessing publications that users recognise and abide by the legal requirements associated with these rights.

**Take down policy:** If you believe that this document breaches copyright, please contact us at [open.research@uwl.ac.uk](mailto:open.research@uwl.ac.uk) providing details, and we will remove access to the work immediately and investigate your claim.

PAPER • OPEN ACCESS

# Extracellular pH monitoring for use in closed-loop vagus nerve stimulation

To cite this article: Simon C Cork *et al* 2018 *J. Neural Eng.* **15** 016001

View the [article online](#) for updates and enhancements.

## Related content

- [A novel flexible cuff-like microelectrode for dual purpose, acute and chronic electrical interfacing with the mouse cervical vagus nerve](#)  
A S Caravaca, T Tsaava, L Goldman *et al.*
- [Vagus nerve stimulation: state of the art of stimulation and recording strategies to address autonomic function neuromodulation](#)  
David Guiraud, David Andreu, Stéphane Bonnet *et al.*
- [Chronic cuffing of cervical vagus nerve inhibits efferent fiber integrity in rat model](#)  
Jesse P Somann, Gabriel O Albors, Kaitlyn V Neihouser *et al.*

## Recent citations

- [An FRET-ICT-based ratiometric fluorescent and colorimetric probe for pH monitoring in lysosomes and water](#)  
Zhang-Yi Li *et al*
- [Tissue Regeneration through Cyber Physical Systems and Microbots](#)  
Prasoon Kumar *et al*
- [Bioelectronic medicine for the autonomic nervous system: clinical applications and perspectives](#)  
Marina Cracchiolo *et al*

# Extracellular pH monitoring for use in closed-loop vagus nerve stimulation

Simon C Cork<sup>1,3</sup> , Amir Eftekhari<sup>2,3</sup>, Khalid B Mirza<sup>2</sup>, Claudio Zuliani<sup>2</sup>, Konstantin Nikolic<sup>2</sup>, James V Gardiner<sup>1</sup>, Stephen R Bloom<sup>1</sup> and Christofer Toumazou<sup>2</sup>

<sup>1</sup> Division of Diabetes, Endocrinology and Metabolism, Section of Endocrinology and Investigative Medicine, Imperial College London, Hammersmith Hospital, London W12 0NN, United Kingdom

<sup>2</sup> Department of Electrical and Electronic Engineering, Institute of Biomedical Engineering, Imperial College London, South Kensington, London SW7 2AZ, United Kingdom

E-mail: [c.toumazou@imperial.ac.uk](mailto:c.toumazou@imperial.ac.uk)

Received 25 April 2017, revised 21 July 2017

Accepted for publication 26 July 2017

Published 1 December 2017



## Abstract

**Objective.** Vagal nerve stimulation (VNS) has shown potential benefits for obesity treatment; however, current devices lack physiological feedback, which limit their efficacy. Changes in extracellular pH ( $pH_e$ ) have shown to be correlated with neural activity, but have traditionally been measured with glass microelectrodes, which limit their *in vivo* applicability. **Approach.** Iridium oxide has previously been shown to be sensitive to fluctuations in pH and is biocompatible. Iridium oxide microelectrodes were inserted into the subdiaphragmatic vagus nerve of anaesthetised rats. Introduction of the gut hormone cholecystokinin (CCK) or distension of the stomach was used to elicit vagal nerve activity. **Main results.** Iridium oxide microelectrodes have sufficient pH sensitivity to readily detect changes in  $pH_e$  associated with both CCK and gastric distension. Furthermore, a custom-made Matlab script was able to use these changes in  $pH_e$  to automatically trigger an implanted VNS device. **Significance.** This is the first study to show  $pH_e$  changes in peripheral nerves *in vivo*. In addition, the demonstration that iridium oxide microelectrodes are sufficiently pH sensitive as to measure changes in  $pH_e$  associated with physiological stimuli means they have the potential to be integrated into closed-loop neurostimulating devices.

**Keywords:** iridium oxide, extracellular pH, neuromodulation, obesity, closed-loop control, vagal nerve stimulation (VNS)

## 1. Introduction

Vagal nerve stimulation (VNS) has been used clinically for many years for the treatment of intractable epilepsy [1]. However, it is becoming increasingly clear that VNS offers potential therapeutic benefit in a number of conditions. One such condition is obesity, where pre-clinical and clinical studies have shown VNS produces moderate weight loss [2–5]. In the

USA, the Federal Drug Administration (FDA) has recently approved the use of VNS for the treatment of obesity.

The role of the vagus nerve in promoting weight loss is well documented. Signals which terminate feeding such as cholecystokinin (CCK) and gastric distension, mediate their effects through interacting with the vagus nerve [6–8], which in turn activates brainstem areas associated with satiety [9]. Sensitivity of the vagus nerve to these satiety signals is reduced in obesity [10] and is believed to be enhanced by VNS [11].

Currently the main limitation with VNS devices (and indeed most brain–technology interfaces), is lack of physiological feedback. Integration of physiological feedback to control stimulation is generally associated with improved therapeutic efficacy [12, 13]. Recording changes in the activity of



Original content from this work may be used under the terms of the [Creative Commons Attribution 3.0 licence](https://creativecommons.org/licenses/by/3.0/). Any further distribution of this work must maintain attribution to the author(s) and the title of the work, journal citation and DOI.

<sup>3</sup> These authors contributed equally to this work.

the vagus nerve associated with satiety signalling, and stimulating it in response to them, may augment the normal physiological signalling of the vagus and increase the efficacy of VNS. However recording such changes remains problematic.

Recording changes in electrical activity of the vagus nerve is one such method by which physiological feedback can be incorporated into VNS devices, however electrical recordings from peripheral nerves tend to be in the  $\mu\text{V}$  range [14], meaning they are hampered by low signal to noise ratio (SNR). In order to compensate for this, individual axons either have to be dissected out of the nerve [15], or the whole nerve removed for *ex vivo* recording [16]. Both methods severely limit the amount of *in vivo* functionality that can be deciphered. It is therefore clear that novel technologies for the detection of changes in neural activity *in vivo* are required for a chronically implanted device.

Previous studies have demonstrated that neural activity correlates with changes in extracellular pH ( $\text{pH}_e$ ) [17–19]. In the *ex vivo* vagus nerve, electrical stimulation results in alkaline  $\text{pH}_e$  shifts of around 0.02 pH units and acid shifts of around 0.05 pH units [18]. Furthermore, in *in vitro* central nervous tissue preparations, depolarisation of neuronal membranes results in  $\text{pH}_e$  changes in both the acidic and alkaline direction [20]. Since  $\text{pH}_e$  changes are recorded directly from within target tissues, they lack interference from distal tissues, providing greater SNR than traditional electrical recordings. However, previous studies examining  $\text{pH}_e$  changes associated with neural activity have significant limitations, in that they have exclusively been performed either *in vitro* or *ex vivo*, and by utilising glass micropipettes to record  $\text{pH}_e$  changes. Due to their fragility and lack of biocompatibility, the use of glass microelectrodes remains unsuitable for incorporation into implantable closed-loop devices. Recent advances in chemical sensing technology and materials have enabled new, stable methods for ionic sensing, especially with pH sensing (for review see [21]). Iridium oxide ( $\text{IrO}_x$ ) has previously been shown to have good pH sensing properties [22] and recently, we described a method for measuring pH in biological tissue using electrodeposited  $\text{IrO}_x$  [23, 24]. An  $\text{IrO}_x$  microwire has the advantage of being rigid, thus allowing easy penetration of the nerve. In addition, iridium is widely used in implantable stimulating electrodes due to its biocompatibility [25]. Sputtering or electrodeposition of iridium oxide is a typical process used in the construction of neural electrical recording electrodes, such as the Utah microelectrode array [26]. Chemical sensing of dopamine has previously been achieved *in vivo* and successfully integrated into closed-loop neurostimulating devices [27], but chemical sensing of the peripheral nervous system *in vivo* has not yet been achieved. Advances in chemical sensing technologies mean it is now possible that  $\text{pH}_e$  recordings could be incorporated into closed-loop neurostimulating devices. However  $\text{pH}_e$  changes in the vagus nerve have not yet been demonstrated *in vivo*.

In this paper, we aimed to determine (a) whether  $\text{IrO}_x$  microelectrodes have sufficient pH sensitivity as to detect changes in  $\text{pH}_e$  in the *in vivo* vagus nerve associated with naturally occurring satiety signals, and (b) whether such changes in  $\text{pH}_e$  could be used for closed-loop VNS.

## 2. Methods

### 2.1. Production of $\text{IrO}_x$ microelectrodes

Iridium wire (0.125 mm temper annealed) was soldered to the exposed end of a covered stainless steel wire. A heat shrink was applied to the exposed connection and Araldite glue applied to each end. After drying, iridium microelectrodes were oxidised in dilute sulphuric acid (0.5 M) using cyclic voltammetry (CHI760E electrochemical workstation, CH Instruments, USA) for 2.5 h.

### 2.2. Calibration of in-house constructed $\text{IrO}_x$ microelectrodes and Utah electrodes

$\text{IrO}_x$  microelectrodes and commercially available Utah array were tested for pH sensitivity using 5 pH buffers (pH4–8). Custom made Matlab code then determined the electrochemical potential of each  $\text{IrO}_x$  microelectrode and Utah array. For *in vivo* studies, only  $\text{IrO}_x$  microelectrodes with a sensitivity of  $>40 \text{ mV/pH}$  were used.

### 2.3. Animals

Male Wistar rats (average weight 350 g, range 300–400 g) were used in all experiments and were obtained from Charles River. All experiments were conducted in accordance with the Animal (Scientific Procedures) Act 1986 and following local ethical approval. Unless otherwise stated, animals were allowed *ad libitum* access to food and water and were maintained on a 12 h light:dark cycle.

### 2.4. pH measurements from subdiaphragmatic vagus

Rats were initially anaesthetised with isoflurane. An intravenous cannula was inserted into the tail vein, through which urethane was slowly infused ( $20 \text{ mg kg}^{-1}$ ) over a period of 25 min, during which isoflurane was slowly reduced to zero. Full anaesthesia was assessed through absence of forepaw pinch reflex. Throughout the procedure, body temperature was monitored via rectal thermistor and maintained at  $37 \pm 1^\circ\text{C}$  (PhysioSuite, Kent Scientific). Heart rate and oxygen saturation were monitored through a pulse oximeter (PhysioSuite, Kent Scientific). Once fully anaesthetised, a midline incision was made in the neck and the trachea exposed, incised and intubated, to allow artificial ventilation (WPI, CW-SAR1000). To record pH changes in the subdiaphragmatic vagus nerve, a midline incision was made in the abdomen, the oesophagus and subdiaphragmatic vagus nerve were exposed and a small thread placed under the vagus. The  $\text{IrO}_x$  microelectrode was inserted into the vagus nerve and the abdominal cavity was filled with warmed paraffin oil. A silver-silver chloride ( $\text{Ag/AgCl}$ ) electrode was placed inside the abdominal cavity to act as a reference.

### 2.5. Cervical stimulation and electrical recording

In a subset of animals ( $n = 13$ ), the ipsilateral vagus nerve was stimulated at the cervical level. The cervical vagus nerve was

exposed using the same midline incision used for ventilation, and a pseudo-tripolar electrode was placed under the nerve. A bipolar platinum electrode was placed inferior to the IrO<sub>x</sub> microelectrode for electrical recording of stimulated compound action potentials (CAPs). Symmetric biphasic pulses of 0.1, 0.2, 0.5 and 1 ms, with currents ranging from 0 to 3 mA were applied to the cervical ipsilateral branch (Keithley 6221 current source, Tektronix, USA), programmed via custom made Matlab script. Each current was iterated 10 times and averaged. Signals were then integrated over bins of 2 ms and a threshold applied (90th percentile of all signals) to detect clusters of A and C fibre activity. C fibre threshold was set at  $2 \text{ m s}^{-1}$ . These strength-duration curves were modelled using Weiss' equation:  $\text{Rheobase} * (1 + \text{Chronaxie}/\text{PW})$ , where PW is the pulse width. In the control case, no electrode was inserted and four strength durations generated. CAPs were recorded using a RHD200 Series amplifier (Intan Technologies, USA) which utilises the multichannel RHD2132 Digital Electrophysiology Interface Chip (gain 45.66 dB, bandwidth 0.2–7.2 kHz). The signal was recorded using Intan's data acquisition software. Bipolar platinum electrodes; similar to those used to record, were placed under the abdominal skin to act as reference electrodes.

## 2.6. CCK studies

In a subset of rats ( $n = 6$ ), CCK at increasing doses ( $50\text{--}300 \text{ pmol kg}^{-1}$ ) was administered to stimulate the vagus nerve. The IrO<sub>x</sub> electrodes were tested prior to and after the experiment to determine their sensitivity. Following introduction of the IrO<sub>x</sub> microelectrode, animals were left to stabilise for 10–15 min. Following baseline pH measurements, CCK-8 (Tocris Bioscience, UK) was dissolved in saline and the required amount drawn into a  $250 \mu\text{l}$  Hamilton syringe, which was back filled with saline. CCK was delivered through the i.v. tail cannula, with a further  $250 \mu\text{l}$  saline used to flush the cannula. A minimum of 15 min was left between subsequent injections.

## 2.7. Gastric distension

In a subset of animals ( $n = 5$ ), gastric inflation was used to stimulate afferent vagal nerve activity. Animals were fasted for 24 h prior to the experiment. Following exposure of the vagus nerve, as detailed above (section 2.4), but prior to insertion of the IrO<sub>x</sub> microelectrode, an 8Fr Foley catheter with 3 ml balloon was inserted into the stomach through the oesophagus, with the balloon positioned inside the stomach. The IrO<sub>x</sub> microelectrode was then inserted into the vagus nerve and the animal was left to stabilise for 10–15 min. Following baseline pH recordings, the balloon was inflated for 3 min with increasing volumes of saline (0.5, 1, 2 and 3 ml), with a minimum of 15 min between inflations.

## 2.8. Data acquisition

pH data was collected from the sensors *in vivo* using commercially available multichannel instrumentation amplifiers, EMF 6 (Lawson Labs Inc, USA), in differential configuration.

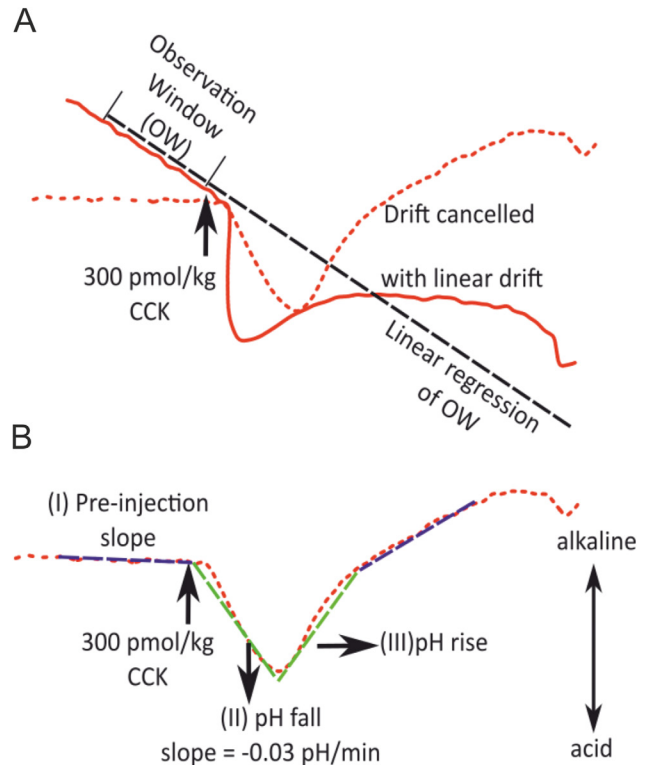


**Figure 1.** (A) The linear estimation of the observation window (OW) is subtracted from the pH waveform to remove linear drift from electrodes. (B) Linear estimation of neural pH waveform in epochs of 1 min. *Epoch (I)* (purple line) shows the pre-injection linear estimation of the pH slope followed by a linear estimation of the fall in pH in *epoch (II)* (green line) which exhibits an approximate slope of  $-0.03 \text{ pH units min}^{-1}$ , in response to  $300 \text{ pmol kg}^{-1}$  CCK. The pH recovers in *epoch (III)* (second purple line) at a relatively slower rate.

The sampling rate of the data acquisition was set at 5 Hz per channel to capture pH changes and safely avoid high frequency electromagnetic or line interference at 50 Hz. The data acquisition and amplifier configuration was performed using customised software provided by Lawson Labs.

## 2.9. Data analysis

The recorded neural pH signal typically consists of inherent drift originating from the open circuit potential of the IrO<sub>x</sub> electrode [28]. This linear drift was negative in almost all instances, and was unidirectional throughout the recording. As part of the post-experiment data analysis procedure, the acquired data was subjected to linear estimation using custom made Matlab script, to account for the linear electrode drift. This was done by selecting an observation window (OW), prior to the injection time. The size of the OW varied between 2 and 5 min dependent on the variance of drift. The size of the OW was chosen from the instance when the stimulus was introduced to point of slope changes. After choosing a suitable OW size, a linear regression was applied on the pre-injection pH waveform. As shown in figure 1(A), the pH waveform, including pre-stimulus pH waveform and the observed pH change in response to the stimulus was subtracted, from the OW linear estimation to subtract background and remove



electrode drift to give an accurate value of the pH change associated to the stimulus.

To calculate relative pH change, baseline pH and peak pH values were obtained by recording the average value of a 5 s window just prior to the stimulus and at peak change. The relative pH change was then calculated by subtracting these values.

### 2.10. Statistical analysis

To determine whether relative changes in pH to a given stimulus were statistically significant, paired *t*-tests were used to compare baseline against peak pH change. A *p* value of  $<0.05$  was considered statistically significant. Values for each stimulus from each animal were then pooled and a one-way ANOVA was used to determine significance between groups.

### 2.11. Code calibration for closed-loop experiments

The data recorded by the EMF 6 was monitored in real time using a Matlab script and converted into pH values from voltage values based on the sensitivity of IrO<sub>x</sub> electrodes measured prior to the experiment. In order to detect the pH change due to CCK injection, the pH waveform was monitored for a period of 5 min pre-injection. This period is referred to as the *code calibration* period. During *code calibration*, a linear estimation was applied to the waveform over OW epochs of 1 min to calculate linear drift/slope of the pH in the nerve. The reason for applying a linear estimation was to apply the transformation between pH and voltage in accordance with the Nernst equation. At the end of the *code calibration* period, the mean slope and the slope standard deviation of 1 min epochs was recorded and CCK was injected. The above method was adopted to mitigate the effect of large non-linear changes in real time.

### 2.12. Detection of pH change for closed-loop stimulation

After *code calibration* (section 2.11) and CCK injection (section 2.6), the pH waveform following injection was also monitored in epochs of 1 min (figure 6(C)), in which the linear regression was applied on the epochs in real time. However, this time, the epoch slope was subtracted from the mean *code calibration* slope to minimise false detection. Previous experiments in which 300 pmol kg<sup>-1</sup> CCK was applied (section 3.3) showed that this dose of CCK produces a change in pH of  $-0.03 \pm 0.01$  pH min<sup>-1</sup> before returning to baseline. At any given time the code ensures that the epoch slopes of the past 2 min and the pH waveform are stored. If the  $\Delta$ pH slope of the previous epoch is negative and its absolute value is  $0.03 \pm 0.01$  pH min<sup>-1</sup>, the code then checks  $\Delta$ pH slope in the subsequent epoch to be positive (i.e. returning to baseline). If this condition is satisfied, then the pH waveform trend is said to be similar to the CCK response trend (figure 6(C)). The stimulation parameters (frequency, pulse width of stimulation, duration of stimulation and stimulation current) having been programmed into the Keithley 6221 current source using the Matlab script prior to injection, and on detection of the

pH slope trend, the Keithley 6221 was signalled to start electrical stimulation. With the above univariate methodology of CCK-pH response detection, there is a minimum delay of 2 min between CCK injection and start of stimulation. At the onset of stimulation, the epoch slopes are not monitored for a period of 15 min before the next CCK injection.

## 3. Results

### 3.1. pH sensitivity of IrO<sub>x</sub> microelectrodes and Utah array

The pH sensitivity of in-house constructed IrO<sub>x</sub> microelectrodes was determined before and after each experiment. Because the Utah array is a validated electrode for clinical use [29, 30], the pH sensitivity of an iridium oxide constructed Utah array was also determined. Figure 2(A) shows the typical pH response slope of a single in-house constructed IrO<sub>x</sub> microelectrode compared to an IrO<sub>x</sub> constructed Utah array. This IrO<sub>x</sub> microelectrode shows a pH sensitivity of  $-75.39 \pm 0.07$  mV/pH unit. In comparison, the Utah array has a slightly lower pH sensitivity of  $-59.9 \pm 4.8$  mV/pH unit. Figure 2(B) shows the average pH sensitivity of a population of IrO<sub>x</sub> microelectrodes before and after experimentation, demonstrating a slight decrease in sensitivity after experimentation ( $-68.78 \pm 5.3$  mV/pH unit versus  $-64.75 \pm 7.94$  mV/pH,  $p < 0.002$ ,  $n = 16$ ).

### 3.2. Nerve integrity testing

Strength duration curves were produced by electrical stimulation of the ipsilateral vagus nerve at the cervical level before and after IrO<sub>x</sub> electrode insertion into the subdiaphragmatic region. Rheobase is a measure of neuronal excitability, and is defined as the minimum current required to depolarise a neuronal membrane. Chronaxie is the minimum time required for a current double the rheobase to depolarise a neuronal membrane. These parameters are governed by the Lapicque equation:

$$I = b \left( 1 + \frac{c}{d} \right).$$

Where *I* relates to current, *b* rheobase, *c* chronaxie and *d* duration.

Rheobase and chronaxie measurements showed no significant alterations in excitation properties (figure 3). Furthermore, latency to activation, fibre type activation and stimulation threshold were unaltered. Control experiments, in which multiple strength duration stimulations were performed in the absence of IrO<sub>x</sub> electrode insertion showed no alterations in nerve responses. This suggests that insertion of the IrO<sub>x</sub> electrodes into the subdiaphragmatic vagus nerve does not result in acute injury to the nerve.

### 3.3. CCK-induced changes in pH<sub>e</sub>

The ability of CCK to produce detectable changes in pH<sub>e</sub> in the subdiaphragmatic vagus nerve was investigated. Intravenous injection of increasing doses of CCK (50, 100, 300 and

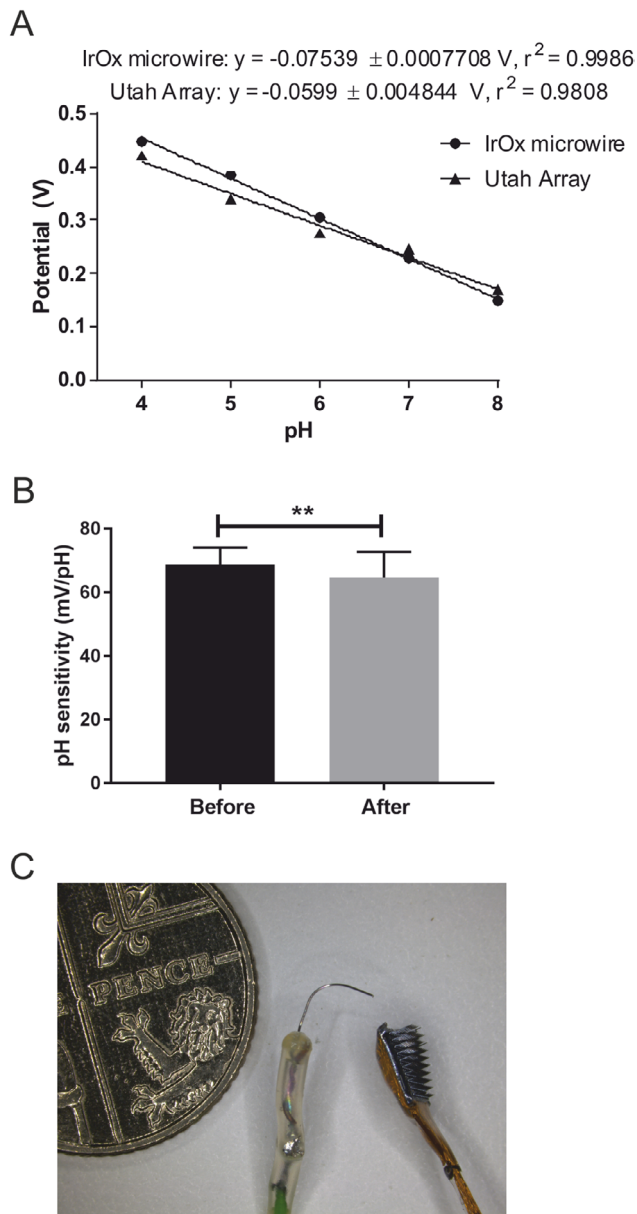


**Figure 2.** (A) Representative calibration curve for in-house constructed iridium oxide microelectrodes (circles) and commercially available Utah array (triangles). Immersion of electrodes in buffers of increasing pH results in a decrease in evoked voltage potential. This individual in-house iridium oxide electrode shows a pH sensitivity of  $-75.39 \pm 0.77 \text{ mV/pH}$  unit, whereas the Utah array shows a slightly lower pH sensitivity of  $-59.9 \pm 4.8 \text{ mV/pH}$  unit. (B) Change in sensitivity of in-house constructed IrO<sub>x</sub> microelectrodes before and after experimentation. Electrodes were calibrated before and after each experiment. After removal from the animal, electrodes show a small but significant decrease in sensitivity (before =  $68.78 \pm 5.306$ , After =  $64.75 \pm 7.94$ ,  $n = 16$ ). (C) Comparison between in-house constructed IrO<sub>x</sub> microelectrodes (left) with commercially available Utah array (right). 5 pence is added for scale (5p = 18 mm diameter). \*\* =  $p < 0.002$ . Bars show mean  $\pm$  SD.

$1000 \text{ pmol kg}^{-1}$ ) produced significant dose-dependent acidosis in the vagus nerve of  $0.014 \pm 0.004 \text{ pH}$  units for  $50 \text{ pmol kg}^{-1}$  to  $0.039 \pm 0.007 \text{ pH}$  units for  $1000 \text{ pmol kg}^{-1}$  (figure 4). In some cases, this acidosis was followed by alkalosis (as observed in figure 6). The decrease in pH started within

15 s of injection, and lasted between 3 and 4 min before returning to baseline. Injection of saline alone did not result in any significant change in  $\text{pH}_e$  (figure 4(E)).

#### 3.4. Gastric distension-induced changes in $\text{pH}_e$

We then determined whether gastric distension produced detectable changes in  $\text{pH}_e$  in the vagus nerve. Small distension volumes ( $0.5\text{--}1 \text{ ml}$ ) produced a reproducible alkalosis of  $0.017 \pm 0.0009$  and  $0.025 \pm 0.003 \text{ pH}$  units respectively (figures 5(A) and (B)). In 55% of cases, larger distension volumes ( $2\text{--}3 \text{ ml}$ ) produced an alkalosis of  $0.05 \pm 0.01$  and  $0.03 \pm 0.004 \text{ pH}$  units respectively (figures 5(C) and (E)), whereas in the remaining 45% of animals, an acidosis was observed of magnitude  $0.05 \pm 0.01 \text{ pH}$  units and  $0.06 \pm 0.01 \text{ pH}$  units for 2 and 3 ml respectively (figures 5(D) and (F)).

#### 3.5. Demonstration of closed-loop capabilities of $\text{pH}_e$ measurements

Finally, we sought to demonstrate that IrO<sub>x</sub>-measured  $\text{pH}_e$  changes in the subdiaphragmatic vagus nerve could be used for closed-loop VNS. Intravenous infusion of  $300 \text{ pmol kg}^{-1}$  CCK produced a significant change in  $\text{pH}_e$  (as described above in section 3.3). Matlab code produced in house automatically identified the shift in pH and triggered a neurostimulator implanted on the ipsilateral cervical vagus nerve (figures 6(A) and (B)). Automatic stimulation of the left vagus nerve was associated with a reduction in heart rate that lasted for the duration of stimulation, before returning to baseline. CCK injection itself was also associated with a modest decrease in heart rate, which has been described previously [31] and was less than that observed for VNS. Stimulation of the ipsilateral vagus nerve also caused profound changes in  $\text{pH}_e$  (likely due to stimulation-induced electrical activity). This lasted for around 10 min before returning to baseline. The detection algorithm is written as such that following positive detection of a CCK-induced  $\text{pH}_e$  change; no further changes are recorded for 15 min. This mitigates the risk of false positive detections caused by stimulation-induced  $\text{pH}_e$  changes.

## 4. Discussion

In this paper we demonstrate a method for recording changes in extracellular pH in the subdiaphragmatic vagus nerve *in vivo*, in the anaesthetised rat. Furthermore we provide evidence that  $\text{pH}_e$  can be incorporated into, and used for closed-loop neurostimulation.

It has been previously documented *in vitro* that electrical activity of neurons is coupled with changes in extracellular pH [17, 18, 20]. Furthermore, IrO<sub>x</sub> has previously been validated as a pH sensor [22, 32], however IrO<sub>x</sub> microelectrodes have never before being applied to the measurement of pH fluxes in peripheral nerves. This has traditionally been achieved through the use of glass micropipettes *ex vivo* nerve preparations. Due to technical limitations, the use of such micropipettes *in vivo* is challenging, and due to their fragility and

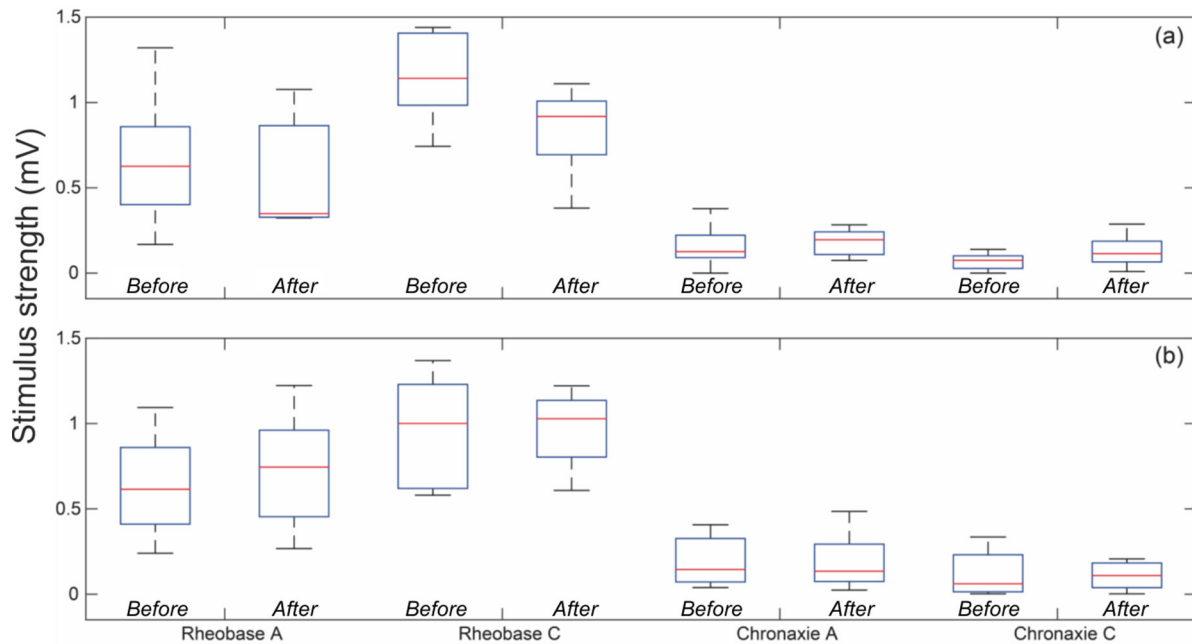


**Figure 3.** Electrical stimulation of the ipsilateral vagus nerve before and after (a) IrO<sub>x</sub> electrode insertion, or without electrode insertion (b). No significant changes were observed in either rheobase or chronaxie measurements following IrO<sub>x</sub> insertion or following repeated stimulation, suggesting acute IrO<sub>x</sub> insertion does not result in significant nerve damage.

inability to be miniaturised, such micropipettes are unsuitable for implantation. Here, we have demonstrated that IrO<sub>x</sub> micro-electrodes are sufficiently sensitive to measure changes in  $\text{pH}_e$  in neuronal tissue *in vivo* caused by physiological stimuli and such changes can be used to drive algorithms for closed-loop neuromodulation.

The vagus nerve is a highly complex nerve, receiving sensory information from both thoracic and abdominal organs. In this regard, signals arising from the gastrointestinal tract can be masked by afferent information arising from cardiorespiratory organs. In order to overcome this issue, we recorded  $\text{pH}_e$  changes specifically from the subdiaphragmatic region of the vagus nerve, which does not receive afferent information from such organs. Furthermore, as this was a proof-of-concept study, animals were artificially ventilated throughout the experiment in order to prevent any changes in spontaneous ventilation which could result in changes in systemic pH. Nevertheless, given the homeostatic mechanisms involved in regulating systemic pH in the conscious animal, we do not anticipate such changes to significantly affect recording accuracy.

Following CCK administration,  $\text{pH}_e$  reliably and reproducibly became more acidic, regardless of the administered dose. This contrasts with gastric distension, whereby small levels of distension (0.5–1 ml) produced alkaline responses, but larger levels of distension (2–3 ml) either produced a biphasic alkaline followed by acidic response, or acidic only. The reasons for this difference in response to the same stimulus across animals are not fully understood, nor are the underlying mechanisms governing  $\text{pH}_e$  changes associated with neural activity. However, both acidic, alkaline and biphasic changes in  $\text{pH}_e$  have been observed by others [33–36]. Kraig *et al* found that repetitive stimulation of the rat cerebellum

often, but not always, resulted in an initial alkaline shift [33]. This initial alkaline shift was blocked by  $\text{Mn}^{2+}$ , a calcium channel blocker, suggesting a role for calcium-induced neuronal activity. In contrast, Chesler and Chen found that stimulation of the turtle cortex *in vitro* resulted in alkalinisation, which lasted for the duration of the stimulus and was also blocked by application of  $\text{Mn}^{2+}$  [36]. The vagus nerve has previously been shown to respond with a brief alkalinisation followed by acidification following stimulation *in vitro*, although no underlying mechanism was investigated [18], however, it has previously been suggested that acidosis could be the result of metabolic acidosis [37]. In our study, we have observed both acidic and alkaline changes in  $\text{pH}_e$  in the vagus nerve in response to two distinct physiological stimuli. In the case of gastric distension, we observed both alkaline shifts and acidic shifts to the same level of stimulus across animals. If the acidification is due to metabolic acidosis, this may represent differences in the ability of the nerve to respond to large stimuli, or may be related to differences in the interaction with afferent fibres communicating gastric distension in the nerve, since these contribute only a minor population [8]. In this paper, we have not sought to add information as to the mechanisms by which  $\text{pH}_e$  changes occur in response to neural activity, but have sought to demonstrate the applicability of  $\text{pH}_e$  to closed-loop neurostimulation. In this demonstration, we used 300 pmol  $\text{kg}^{-1}$  CCK as the stimulus, which produces reproducible changes in  $\text{pH}_e$ , with a characteristic shape, slope and peak  $\text{pH}_e$  change across animals. Through this, the detection algorithm could be ‘trained’ to detect this characteristic change in  $\text{pH}_e$ , thus reducing the chances of false-positive detections. The different responses in  $\text{pH}_e$  associated with gastric distension produce an obvious limitation to the algorithm design, however provided the response is maintained in



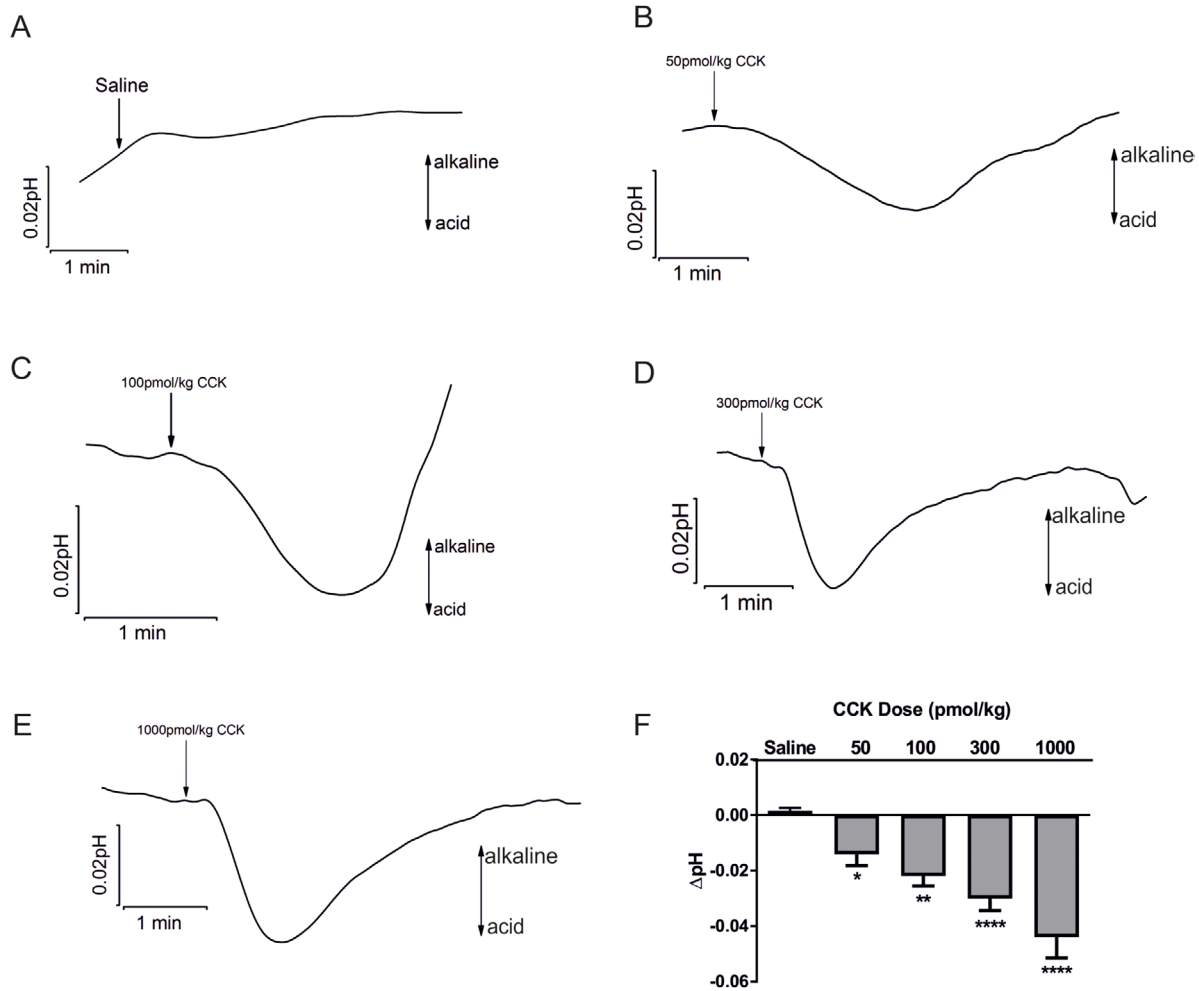
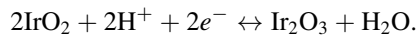


**Figure 4.** (A)–(E) Saline and CCK-induced changes in  $\text{pH}_e$  in the subdiaphragmatic vagus nerve with intravenous administration of increasing doses of CCK (50–1000  $\text{pmol kg}^{-1}$ ,  $n = 6$  animals). (F) Average peak changes in  $\text{pH}_e$  in response to increasing doses of CCK. One-way ANOVA revealed significant changes in  $\text{pH}_e$  in all doses against equi-volume administration of saline alone. \* =  $p < 0.05$ , \*\* =  $p < 0.001$ , \*\*\*\* =  $p < 0.0001$  versus saline.

each individual animal, it is possible that the algorithm could be trained in the same manner.

The electrochemical potential of iridium oxide in a solution depends mainly on the pH of the media, since an electrochemical equilibrium between the iridium oxide and the  $\text{H}^+$  ions is established as described by the following equation:



This equilibrium is governed by the Nerst equation:

$$E = E_0 + \frac{RT}{nF} \log_{10}(C_{\text{H}}) = E_0 - 0.059 \text{ pH}.$$

This equation predicts that the electrochemical potential of the iridium oxide electrodes changes linearly with the pH with a typical slope of  $-59 \text{ mV/pH}$  unit. In reality, interfacial equilibrium is slightly more complex which accounts for larger slopes, typically ranging from  $-59$  to  $-90 \text{ mV/pH}$  unit depending on the preparation protocols. Using our protocols, we demonstrate a pH sensitivity of  $-68.78 \pm 5.3 \text{ mV/pH}$  unit. The differences between measured and theoretical pH sensitivities of  $\text{IrO}_x$  are dependent upon the reduction state of the anodic iridium oxide film, with the reduced state having more

acidic properties than the oxidised form [38] and are therefore influenced by oxidising paradigm and efficiency.

Recording neural activity has become a major challenge in the expanding field of neuro-technology. Electrical recording from within neural tissue offers significantly enhanced spatiotemporal resolution when compared to non-invasive techniques (e.g. fMRI, EEG) [39]. However recordings from peripheral nerves are especially associated with interference from neighbouring electrically dependent processes (e.g. heart rate, respiration, muscle movement) [40]. Small electrical signals produced by peripheral nerves, as well as the presence of interfering bioelectrical signals from distal tissues within the bandwidth of interest, produce challenges for electronic front-ends and interfaces [41]. We sought to overcome these limitations by recording chemical changes associated with nerve activity. Chemical signals have significantly higher amplitude (tens of millivolts) and hence better SNR compared with traditional electrical recordings. The chemical signals also have lower bandwidth, hence making them easy to separate from interferences such as cardiorespiratory signals. In the context of the vagus nerve, we have demonstrated that chemical neural recordings can be used as a viable means of detecting

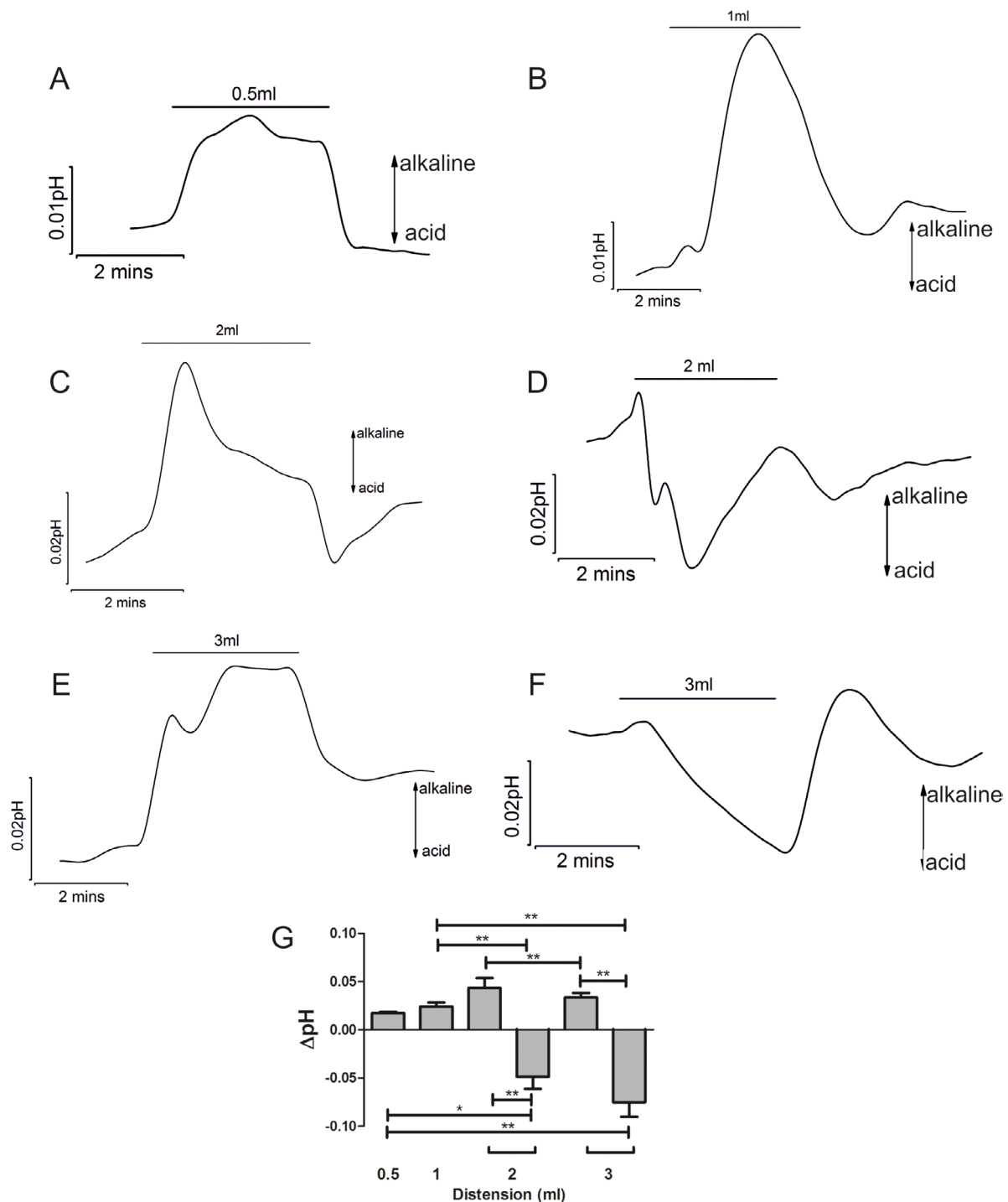


**Figure 5.** Distension-induced changes in  $pH_e$  in the subdiaphragmatic vagus nerve ((A)–(D), 0.5–3 ml). Small levels of distension (A) and (B) produce an alkaline shift in  $pH_e$ . Higher levels of distension produce both biphasic (C), acidotic (D) and (F) and alkaline (E) shifts in  $pH_e$ . (G) Average peak change in  $pH_e$  for each level of distension (\* =  $p < 0.05$ , \*\* =  $p < 0.01$ ,  $n = 5$  animals). Lines denote duration of distension.

changes in neural activity as a result of physiological events. We have also demonstrated that neural  $pH_e$  changes observed in relation to CCK and gastric distension have characteristic shapes and follow dose-response relationships.

In order to further increase spatial resolution of neural recordings, various laboratories have developed high density multielectrode arrays (MEAs), with large numbers of individually addressable spikes. Many of these MEAs have the added benefit of varying spike length, offering further spatial

resolution. One such device is the commercially available Utah electrode array (UEA), which is constructed from either platinum or iridium oxide. Because of its construction from  $IrO_x$ , and its previous use in clinical applications [29, 30], we further provided evidence that the UEA has pH sensing capabilities. The development of a slanted UEA for use in peripheral nerves [26], further increases the possibility that devices such as the UEA can be used for human  $pH_e$  nerve recordings.

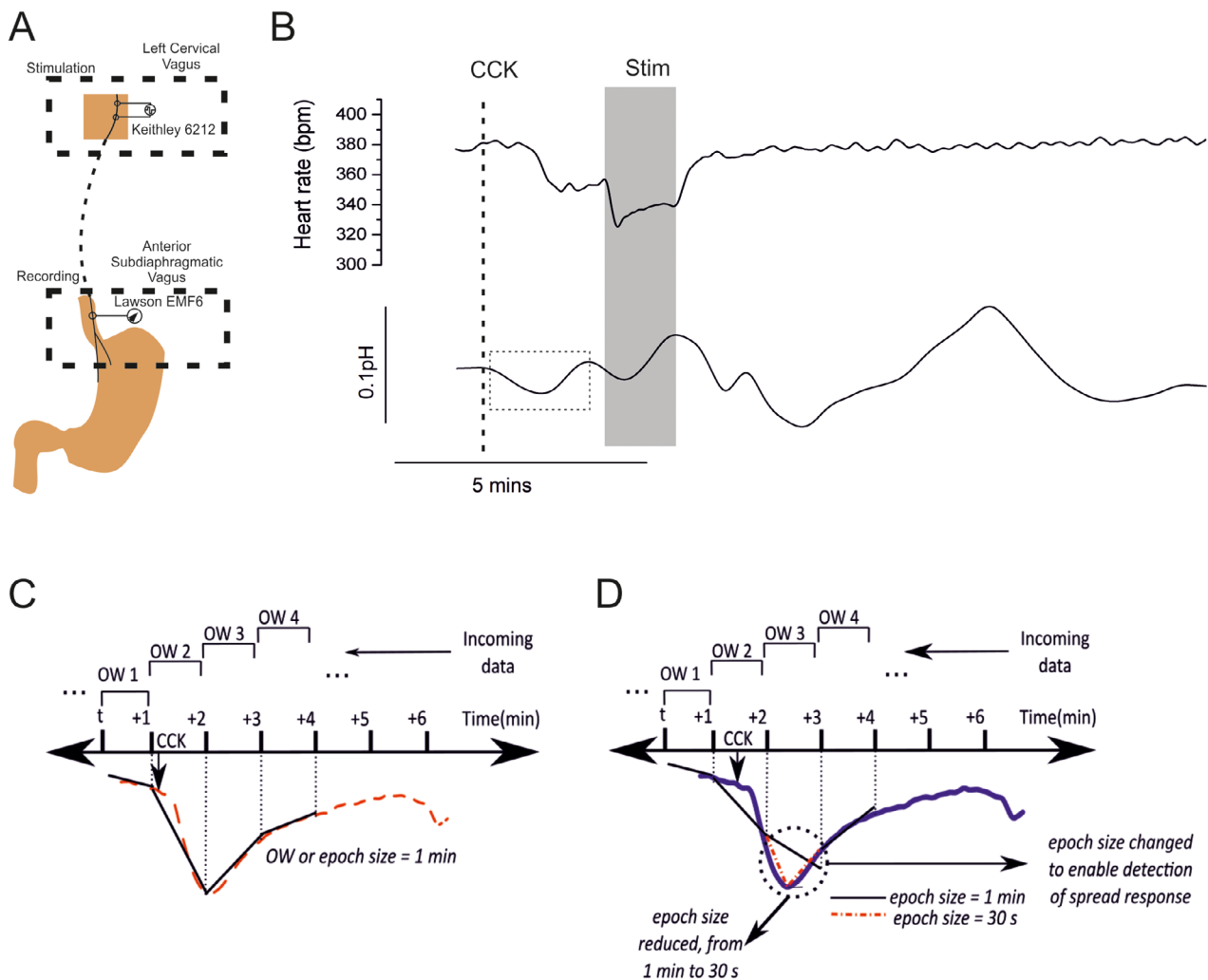


**Figure 6.** Demonstration of the closed-loop capabilities of  $\text{pH}_e$  monitoring using  $\text{IrO}_x$  microelectrodes in anaesthetised rats. (A)  $\text{IrO}_x$  microelectrodes were inserted into the subdiaphragmatic vagus nerve and stimulator implanted on ipsilateral cervical vagus nerve. (B)  $300 \text{ pmol kg}^{-1}$  CCK injected intravenously (dashed line), produces a characteristic decrease in  $\text{pH}_e$  (boxed area) and a small drop in heart rate. The drop in  $\text{pH}_e$  is detected by custom made Matlab script and triggers the implanted stimulator (grey line). (C) Schematic representation of custom made Matlab script. Script reads data in 1 min epochs, with a decrease of  $0.03 \pm 0.01 \text{ pH min}^{-1}$  in OW2 against OW1, followed by an increase in  $\text{pH}_e$  of the same magnitude in OW3 is recognised as a positive CCK-induced  $\text{pH}_e$  change. (D) should the introduction of CCK occur in the middle of an OW, the OW window is automatically reduced to 30 s.  $N = 11$  animals.

## 5. Conclusions

VNS has been shown to produce moderate effects on weight loss using current ‘open-loop’ technologies [2, 5, 42]. The addition of physiological feedback to create closed-loop VNS devices has been shown to offer greater efficacy [43, 44]. We provide a novel approach to providing physiological feedback to VNS devices, through the use of extracellular pH changes associated with neural activity. Furthermore, the use of  $\text{pH}_e$  for the control of neural implants extends further than peripheral nervous tissues, and has the potential to integrate into central brain structures. The characteristic shape of neural pH change, its proportionality to dosage, ease of separation from interfering signals, the possibility to record neural  $\text{pH}_e$  using  $\text{IrO}_x$ , (which is a biocompatible material and has an established fabrication procedure), and the demonstration that  $\text{pH}_e$  can be used in a closed-loop paradigm, demonstrates that

chemical neural recording has the potential of being used as a viable neurotechnology within closed-loop implants.

## Acknowledgments

We thank Drs Nir Grossman, Agnieszka Falinska, Andrea Alenda and Mr Nishanth Kulasekaram for technical and intellectual assistance.

This article presents independent research funded by a European Research Council (ERC) Synergy Grant (Grant ref: 319818—i2MOVE) at Imperial College London. The views expressed are those of the author(s) and not necessarily those of the ERC.

The Section of Endocrinology and Investigative Medicine is funded by grants from the MRC, BBSRC, NIHR, an Integrative Mammalian Biology (IMB) Capacity Building Award, an FP7-HEALTH-2009-241592 EuroCHIP grant

and is supported by the NIHR Biomedical Research Centre Funding Scheme.

## Author contributions

AE, SRB and CT conceived the project. SCC performed *in vivo* pH recordings and closed-loop stimulation recordings. AE and KBM produced Matlab scripts for data analysis. KBM produced Matlab scripts for closed-loop VNS. CZ developed the protocol for IrOx microelectrode production. SCC wrote the manuscript with input from all authors. KN, JVG, SRB and CT directed the project. JVG, SRB and CT directed the project.

## Competing financial interests

CT holds a patent on chemical monitoring of the vagus nerve (US9055875 B2). All other authors declare no competing financial interests.

## ORCID iDs

Simon C Cork  <https://orcid.org/0000-0001-5720-9751>

## References

- [1] Yuan H and Silberstein S D 2016 Vagus nerve and vagus nerve stimulation, a comprehensive review: part II *Headache* **56** 259–66
- [2] Burneo J G, Faught E, Knowlton R, Morawetz R and Kuzniecky R 2002 Weight loss associated with vagus nerve stimulation *Neurology* **59** 463–4
- [3] Apovian C M, Shah S N, Wolfe B M, Ikramuddin S, Miller C J, Tweden K S, Billington C J and Shikora S A 2017 Two-year outcomes of vagal nerve blocking (vBloc) for the treatment of obesity in the recharge trial *Obesity Surg.* **27** 169–76
- [4] Banni S *et al* 2012 Vagus nerve stimulation reduces body weight and fat mass in rats *PLoS One* **7** e44813
- [5] Sarr M G *et al* 2012 The EMPOWER study: randomized, prospective, double-blind, multicenter trial of vagal blockade to induce weight loss in morbid obesity *Obesity Surg.* **22** 1771–82
- [6] Dockray G J 2013 Enteroendocrine cell signalling via the vagus nerve *Curr. Opin. Pharmacol.* **13** 954–8
- [7] Rogers R C and Hermann G E 2008 Mechanisms of action of CCK to activate central vagal afferent terminals *Peptides* **29** 1716–25
- [8] Williams E K, Chang R B, Strohlic D E, Umans B D, Lowell B B and Liberles S D 2016 Sensory neurons that detect stretch and nutrients in the digestive system *Cell* **166** 209–21
- [9] Browning K N, Verheijden S and Boeckxstaens G E 2017 The vagus nerve in appetite regulation, mood, and intestinal inflammation *Gastroenterology* **152** 730–44
- [10] Daly D M, Park S J, Valinsky W C and Beyak M J 2011 Impaired intestinal afferent nerve satiety signalling and vagal afferent excitability in diet induced obesity in the mouse *J. Physiol.* **589** 2857–70
- [11] Cunningham J T, Mifflin S W, Gould G G and Frazer A 2008 Induction of c-Fos and DeltaFosB immunoreactivity in rat brain by vagal nerve stimulation *Neuropsychopharmacology* **33** 1884–95
- [12] Guiraud D *et al* 2016 Vagus nerve stimulation: state of the art of stimulation and recording strategies to address autonomic function neuromodulation *J. Neural Eng.* **13** 041002
- [13] Wright J, Macefield V G, van Schaik A and Tapsen J C 2016 A review of control strategies in closed-loop neuroprosthetic systems *Front. Neurosci.* **10** 312
- [14] Nikolic Z M, Popovic D B, Stein R B and Kenwell Z 1994 Instrumentation for ENG and EMG recordings in FES systems *IEEE Trans. Biomed. Eng.* **41** 703–6
- [15] Schwartz G J, McHugh P R and Moran T H 1991 Integration of vagal afferent responses to gastric loads and cholecystokinin in rats *Am. J. Physiol.* **261** R64–9
- [16] Birrell M A, Crispino N, Hele D J, Patel H J, Yacoub M H, Barnes P J and Belvisi M G 2002 Effect of dopamine receptor agonists on sensory nerve activity: possible therapeutic targets for the treatment of asthma and COPD *Br. J. Pharmacol.* **136** 620–8
- [17] Chesler M and Kaila K 1992 Modulation of pH by neuronal activity *Trends Neurosci.* **15** 396–402
- [18] Endres W, Grafe P, Bostock H and Ten Bruggencate G 1986 Changes in extracellular pH during electrical stimulation of isolated rat vagus nerve *Neurosci. Lett.* **64** 201–5
- [19] Tong C K and Chesler M 1999 Activity-evoked extracellular pH shifts in slices of rat dorsal lateral geniculate nucleus *Brain Res.* **815** 373–81
- [20] Makani S and Chesler M 2010 Rapid rise of extracellular pH evoked by neural activity is generated by the plasma membrane calcium ATPase *J. Neurophysiol.* **103** 667–76
- [21] Ronkainen N J, Halsall H B and Heineman W R 2010 Electrochemical biosensors *Chem. Soc. Rev.* **39** 1747–63
- [22] Vanhoudt P, Lewandowski Z and Little B 1992 Iridium oxide pH microelectrode *Biotechnol. Bioeng.* **40** 601–8
- [23] Zuliani C, Ng F S, Alenda A, Eftekhari A, Peters N S and Toumazou C 2016 An array of individually addressable micro-needles for mapping pH distributions *Analyst* **141** 4659–66
- [24] Mirza K B, Zuliani C, Hou B, Ng F S, Peters N S and Toumazou C 2017 Injection moulded microneedle sensor for real-time wireless pH monitoring *IEEE Engineering in Medicine and Biology (Seoul, Republic of Korea)*
- [25] Lee I S, Whang C N, Choi K, Choo M S and Lee Y H 2002 Characterization of iridium film as a stimulating neural electrode *Biomaterials* **23** 2375–80
- [26] Wark H A *et al* 2013 A new high-density (25 electrodes mm<sup>-2</sup>) penetrating microelectrode array for recording and stimulating sub-millimeter neuroanatomical structures *J. Neural Eng.* **10** 1088
- [27] Bozorgzadeh B, Schuweiler D R, Bobak M J, Garris P A and Mohseni P 2016 Neurochemostat: a neural interface SoC with integrated chemometrics for closed-loop regulation of brain dopamine *IEEE Trans. Biomed. Circuits Syst.* **10** 654–67
- [28] Ges I A, Ivanov B L, Schaffer D K, Lima E A, Werdich A A and Baudenbacher F J 2005 Thin-film IrO<sub>x</sub> pH microelectrode for microfluidic-based microsystems *Biosens. Bioelectron.* **21** 248–56
- [29] Hochberg L R, Serruya M D, Friehs G M, Mukand J A, Saleh M, Caplan A H, Branner A, Chen D, Penn R D and Donoghue J P 2006 Neuronal ensemble control of prosthetic devices by a human with tetraplegia *Nature* **442** 164–71
- [30] Normann R A and Fernandez E 2016 Clinical applications of penetrating neural interfaces and Utah electrode array technologies *J. Neural Eng.* **13** 061003
- [31] Kurosawa M, Iijima S, Funakoshi A, Kawanami T, Miyasaka K, Bucinskaite V and Lundberg T 2001



- Cholecystokinin-8 (CCK-8) has no effect on heart rate in rats lacking CCK-A receptors *Peptides* **22** 1279–84
- [32] Kakooei S, Ismail M C and Ari-Wahjoedi B 2013 An overview of pH sensors based on iridium oxide: fabrication and application *Int. J. Mater. Struct. Innov.* **1** 62–72
- [33] Kraig R P, Ferreira-Filho C R and Nicholson C 1983 Alkaline and acid transients in cerebellar microenvironment *J. Neurophysiol.* **49** 831–50
- [34] Urbanics R, Leniger-Follert E and Lubbers D W 1978 Time course of changes of extracellular  $H_+$  and  $K_+$  activities during and after direct electrical stimulation of the brain cortex *Pflugers Arch.* **378** 47–53
- [35] Xiong Z Q and Stringer J L 2000 Extracellular pH responses in CA1 and the dentate gyrus during electrical stimulation, seizure discharges, and spreading depression *J. Neurophysiol.* **83** 3519–24
- [36] Chesler M and Chan C Y 1988 Stimulus-induced extracellular pH transients in the *in vitro* turtle cerebellum *Neuroscience* **27** 941–8
- [37] Chesler M 2003 Regulation and modulation of pH in the brain *Physiol. Rev.* **83** 1183–221
- [38] Olthuis S, Robben M A M, Bergveld P, Bos M and van der Linden W E 1990 pH sensor properties of electrochemically grown iridium oxide *Sensors Actuators B* **2** 247–56
- [39] Gunasekera B, Saxena T, Bellamkonda R and Karumbaiah L 2015 Intracortical recording interfaces: current challenges to chronic recording function *ACS Chem. Neurosci.* **6** 68–83
- [40] Ortiz-Catalan M, Marin-Millan J, Delbeke J, Hakansson B and Branemark R 2013 Effect on signal-to-noise ratio of splitting the continuous contacts of cuff electrodes into smaller recording areas *J. Neuroeng. Rehabil.* **10** 22
- [41] Raspopovic S, Carpaneto J, Udina E, Navarro X and Micera S 2010 On the identification of sensory information from mixed nerves by using single-channel cuff electrodes *J. Neuroeng. Rehabil.* **7** 17
- [42] Ikramuddin S et al 2014 Effect of reversible intermittent intra-abdominal vagal nerve blockade on morbid obesity: the ReCharge randomized clinical trial *JAMA* **312** 915–22
- [43] Bohdjalian A, Prager G, Aviv R, Policker S, Schindler K, Kretschmer S, Riener R, Zacherl J and Ludvik B 2006 One-year experience with Tantalus: a new surgical approach to treat morbid obesity *Obesity Surg.* **16** 627–34
- [44] Horbach T, Thalheimer A, Seyfried F, Eschenbacher F, Schuhmann P and Meyer G 2015 Abiliti closed-loop gastric electrical stimulation system for treatment of obesity: clinical results with a 27 month follow-up *Obesity Surg.* **25** 1779–87